Medical Image Registration and Applications: Final project report

Alejandro Cortina Uribe
EMJMD in Medical Imaging and Applications
Universitat de Girona
Girona, Spain
acortinau@gmail.com

Vladyslav Zalevskyi
EMJMD in Medical Imaging and Applications
Universitat de Girona
Girona, Spain
zalevskyi.vladyslav@gmail.com

***Abstract*—In this project, we implemented and tested different approaches to register lung CT scans (inhale and exhale) from the DIR Lab COPDGene dataset. The first one consisted of an intensity-based image registration algorithm, using a normalized correlation criterion with an optimization procedure. By using Elastix, we combined an affine and two nonrigid B-spline transformations in a multi-resolution framework. We achieved a mean target registration error (TRE) of 1.5816 $\pm$ 0.64 mm, for the dataset cases COPD1 to COPD4. The second approach consisted of using a pre-trained deep learning model based on SynthReg. From the original model, which was trained in a contrast-agnostic manner, we adapted the sm-shapes instance which we used to obtain a deformation map. With this model, we obtained a mean TRE of 15.224 $\pm$ 4.096 mm for the same cases. Finally, we implemented an automated registration pipeline using the first approach, which was used on the day of the challenge to register three new test cases (COPD0, COPD5, and COPD6). On said challenge day, we obtained a mean TRE of 1.423 mm.**

***Index Terms*—lung, registration, deep learning**

I. Introduction

The registration between two medical images is used for diverse applications such as atlas creation, intra-patient scan alignment, segmentation, volume quantification, etc., that aid clinicians in disease diagnosis, staging, and treatment. For chronic obstructive pulmonary disease (COPD), lung CT images have arisen to be helpful for disease diagnosis and characterization [9]. As COPD can appear widely variable in a person it is often misdiagnosed or overlooked during the medical evaluation, which is why it is important to gather as much information as possible coming from clinical symptoms, genetic information and CT imaging studies [7].

The COPDGene Study has been developed to accurately diagnose COPD, and it is one of the largest studies to investigate underlying genetic factors of this disease. Specifically, CT scans are used to quantify the extent of emphysema, airway wall thickening and air trapping; and for these tasks, the registration between maximum inhale and exhale phases is a key element [1].

II. Materials and Methods

The DIR Lab COPDGene [1] dataset contains 10 pairs of Lung CT scans, from which we used cases 1 to 4 as training data to develop our approaches. Each pair contains maximum inhalation and exhalation scans. Along with the images, a file containing 300 landmarks for each of the phases is given. The original images are given in a raw format, without any type of metadata other than the image dimensions (voxel units) and voxel dimensions (millimeters). The landmarks files contain the coordinates of each point and the mean displacement (millimeters) between the two sets. We used the software ITK-Snap (version 3.6.0) to read each file and correct its orientation, from RAI (Right-Left, Anterior-Posterior, Inferior-Superior) to RAS (Superior-Inferior). Also, we assessed the coordinates given in the landmarks files in order to match them correctly for further point transformations. In figure 1, we can see an example of inhale and exhale landmarks plotted on the original image.

A. Intensity-based registration using Elastix

Elastix provides a framework to deploy intensity-based registration with different transformations. It is based on the traditional scheme of finding the best transformation that optimizes a similarity metric between the fixed and moving images, through an iterative process. It also provides the option to implement a multi-resolution registration through image pyramid schedules and to define many other components such as the interpolator, optimizer, metric, number of iterations, number of spatial samples, etc. We developed our experiments in a sequential manner, starting from the simple default parameters provided by Elastix, and finishing with more complex task-specific publicly-available parameter maps (see section III Experiments and Results). The code used to run all this experiments can be accessed at https://github.com/Vivikar/lung-ct-registration.

1) Pre-processing: By analyzing the images, we notice that they had a circular FOV with a voxel intensity value of -2000, which does not correspond to the actual image and should not be taken into account when normalizing or applying any pre-processing algorithm. It is also worth noting that the voxel intensity range does not fall directly in the Houndsfield Units (HU) range so whenever it would be necessary we performed intensity normalization by subtracting the value 1024 (more in the next section II-A2). We selected this number based on the default known values for HU transformation when the slope and intercept values are not available (i.e. the file is not DICOM). Furthermore, we tested different contrast-enhancing

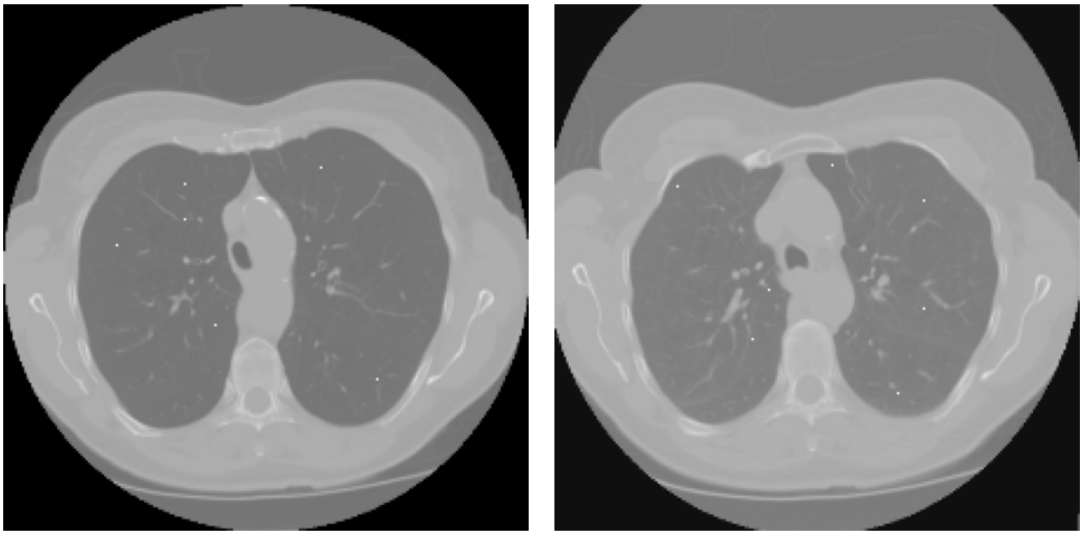

Fig. 1. Landmark points plotted over the original image (white dots). Case image 1, transversal view, left-inhale, right-exhale.

algorithms and evaluate their impact on the registration performance. We performed histogram equalization and contrast limited adaptive histogram equalization (CLAHE). The latter is an algorithm for local contrast enhancement, where histograms are computed on different tiles of the image. In figure 2 we can see an example of these histogram equalization techniques.

2) Lung segmentation: Elastix allows us to use a binary mask when setting up the registration components. This mask is used to limit the region where the samples are drawn, thus restricting the influence of non-interesting regions. In the case of lung registration, this mask comes very handy for two main reasons: the lung mask can be helpful to first affinely register them and then focus on performing non-rigid registration inside the lungs and neglect the static rib cage structure. For these reasons, we implemented and tested two lung segmentation algorithms, a thresholding-based approach and a deep learning one.

For the first algorithm, we carried out classic image processing techniques starting with histogram thresholding using Otsu, and then post-process each slice with connected components and morphological operations. A final 3D connected components algorithm is used to remove small spots. An advantage of this algorithm is that it is relatively fast ($<$ 1 min) but the segmentation includes the trachea, which is not part of the lungs. An example of the lung mask can be seen in figure 3-a. For the second algorithm, we used a pre-trained U-Net for lung segmentation [6]. As this model was trained with CT scans in the HU range, we normalized our images as described previously before feeding them to the model. Simple post-processing leads to excellent only-lung segmentation (figure 3-b). The computation time for this algorithm was an average of 100 seconds, depending on the CPU specifications where the algorithm is run.

3) Registration components: Intensity-based similarity metrics are widely used for image registration, from the classic sum of square differences (SSD) to advanced mattes mutual information. For lung registration, the chosen metric should work under the assumption that the voxel intensity does not remain constant in the fixed and moving images. This is due to the reduction of lung density during the inhaling phase caused by the inflow of air [9]. In the end, this phenomenon translates into the decrease of HU in the parenchymal region, as can be seen in figure 4.

We chose then to use the normalized correlation coefficient (NCC) as a similarity metric (eq 1), which is invariant to linear differences between intensity distributions [10]. Where I and T are the two images being correlated, M and N are the dimensions of the images, and μ_I and μ_T are the mean intensities of the images I and T, respectively.

$$\frac{\sum_{i=1}^{M}\sum_{j=1}^{N}(I(i,j)-\mu_I)(T(i,j)-\mu_T)}{\sqrt{\sum_{i=1}^{M}\sum_{j=1}^{N}(I(i,j)-\mu_I)^2}\sqrt{\sum_{i=1}^{M}\sum_{j=1}^{N}(T(i,j)-\mu_T)^2}} \tag{1}$$

From the publicly available parameter maps of ElastixModelZoo, we used parameter map 11. In the corresponding to it paper [10], the authors implemented three consecutive transformations, affine and two non-rigid b-splines to register successfully inspiration and expiration scans from the EMPIRE10 challenge.

Using their parameter map as a baseline, we modified the image pyramid schedule and the number of samples. As our images do not have isotropic voxels we decided to modify the blurring degree (sigma) of the third dimension in the multi-resolution pyramid, as recommended in the documentation. We ended up using five resolutions with the schedule 16 16 4 8 8 3 4 4 2 2 2 1 1 1 1. Also, to improve the registration

Fig. 2. Preprocessing examples. Left- original image, center- equalized histogram, right- CLAHE.

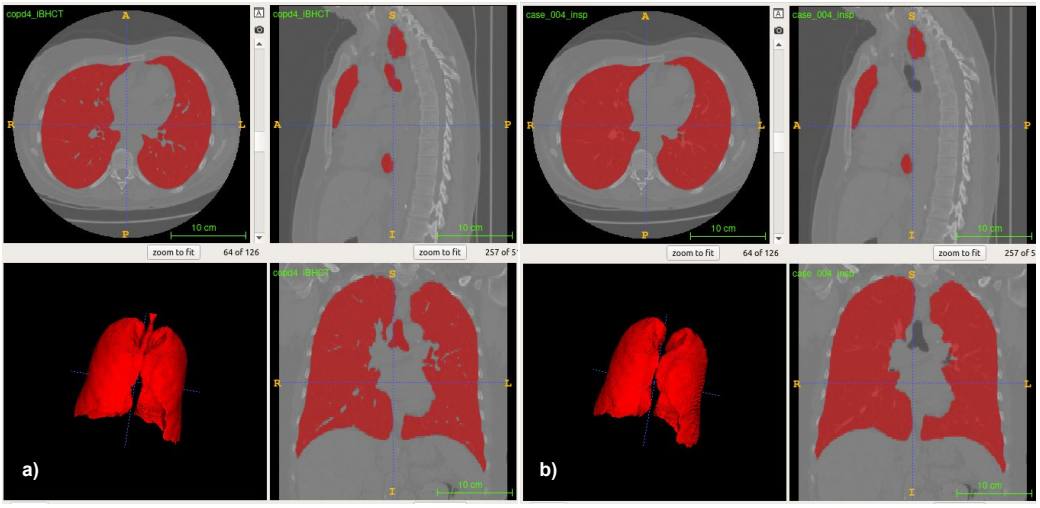

Fig. 3. Lung masks examples. a) Threshold-base algorithm, b) U-Net algorithm.

performance at the expense of a larger computational time, we increased the number of samples to compute the metric at each resolution to 10000.

B. Registration using deep learning model

There are several state-of-the-art deep learning (DL) models that perform the registration of two images with a learning-based approach. In [3] they implemented an improvement of the VoxelMorph model with two general steps, first obtain a coarse heatmap prediction through keypoint correspondences after self-supervised training, and then refine it with non-local MIND loss and single-instance optimization. The same authors also proposed a new architecture GraphRegNet [2], based on convolutional graph neural network layers with the goal of tackling the large 3D deformations limitations that current DL models face. Another way to tackle the previous issue is to implement a multi-resolution framework like they did in [4], where a 3-level structure of CNN's is trained along anatomical priors (lung lobes segmentations) and using the normalized gradient field distance as loss function.

But many DL models still do not generalize to different data-type inputs, meaning that when feeding new images different to the distribution the model was trained with, it will fail to register them. SynthMorph [5] tried to solve this issue by training a model with synthetic data that is beyond the realistic range of medical images, to encourage networks to generalize to the different contrasts and modalities. From this model, we chose to use the shapes variant that was trained to predict a deformation field between a pair of images with random shapes (figure 5). This model is a basic VoxelMorph U-Net that predicts a diffeomorphic deformation field and was trained in an unsupervised manner optimizing the dice-based loss of the deformed shapes overlap. Our main objective to use

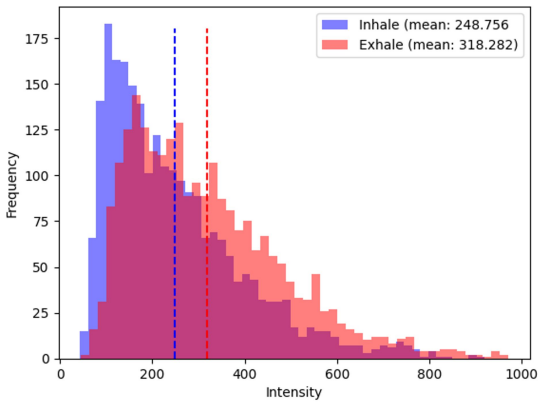

Fig. 4. Histograms of voxel intensities in 3x3 neighborhood around all 300 landmarks, for inhale and exhale images of case 1.

this model was to test the power of contrast-agnostic models, and specifically, to test how well this model performs even when it has not been trained with any real medical images.

1) Pre-processing: In order for us to use the pre-trained model we needed to perform a series of preprocessing tasks to our images, following the recommendations from the authors. It is important to mention that since the model was originally purposed for brain MRI scans, for certain tasks we needed to manually experiment and set hyperparameters for the model to perform as desired.

We first perform basic registration with translation and affine transformations between the fixed and moving images, and with the transformation parameter map we propagate the segmentation mask and transform the original landmarks, thus moving all required data to the same space. Then, the fixed and moving images are scaled using min-max. Finally, since each case images have different dimensions and voxel spacing, in order for us to feed them to the U-Net, we resize them to size 224, 224, 96 by changing the voxel spacing. We found empirically that this size works the best for the model since each dimension is divisible by 2^5, 5 being the number of max pooling layers inside the U-Net. Lastly, after transforming the landmarks to the new resampled dimensions for proper TRE computation, we obtained the prepared data for the SynthMorph inference experiments.

III. Experiments and Results

In this section, we describe the experiments we implemented and show tables with their results, for each of the two approaches. In order to evaluate the registration results, we use the landmark points from both phases and calculate the average euclidean distance between them, called target registration error (TRE).

A. Intensity-based registration using Elastix

The goal was to register the inhale image to the exhale one, but it is important to remark that, in order for us to use Elastix to transform the points the registration transformation should be inverse. Thus, we decided to inverse the transformation from the beginning by selecting the moving and fixed images as the exhale and inhale scans, respectively. We assessed the computation time for each group of experiments.

To evaluate how the generic transformations from Elastix perform on this problem we set up a series of experiments using the circular FOV (or cylinder mask) as the registration mask (table 1). These generic transformations constitute in general the following registration components: advanced mattes mutual information as similarity metric, 4 resolutions, advanced stochastic gradient descent as an optimizer, and 2048 spatial samples, amongst others.

- **Baseline**. No registration.
- **1a**. Affine transformation.
- **1b**. Affine + b-spline.
- **1c**. Euclidean + Affine + b-spline.

Following these experiments, we noticed that first aligning the images with affine transformation and then performing more precise non-rigid transformation works the best (1c). To test the influence of the lung mask in the non-rigid b-spline transformation, we ran another experiment (table I).

- **2a**. Euclidean + affine using cylinder mask, followed by b-spline using lung mask.

We implemented then the parameter maps 11 [10] in a series of experiments to test the best combination of the three available parameter maps (affine, b-spline 1, b-spline 2) with the two masks (cylinder and lung) (table II).

- **3a-I**. Affine + b-spline 1 using only cylinder mask.
- **3a-II**. Affine + b-spline 2 using only clylinder mask.
- **3b-I**. Affine with cylinder mask, followed by b-spline 1 with lung mask.
- **3b-II**. Affine with cylinder mask, followed by b-spline 2 with lung mask.

And to adapt the paper's implementation [10] to our problem we performed a final experiment in a similar manner, by using only the lung mask for the second b-spline.

- **3c**. Affine and b-spline 1 with cylinder mask, followed by b-spline 2 with lung mask.

We decided to also run an experiment using directly the lung mask and the b-spline 1 parameter map from [10]. Also, we tested on this simpler framework the influence of changing specific registration components, as well as the contrast-enhancing techniques (table III). Below we report the components that led to the most relevant results.

- **4a**. Changing the number of spatial samples to 10000.
- **4b**. Changing the image pyramid schedule to 16 16 4 8 8 3 4 4 2 2 2 1 1 1 1.
- **4c**. Changing both the number of spatial samples and the pyramid schedule.
- **4d**. 4c setting with CLAHE as pre-processing.
- **4e**. 4c setting with histogram equalization as pre-processing.

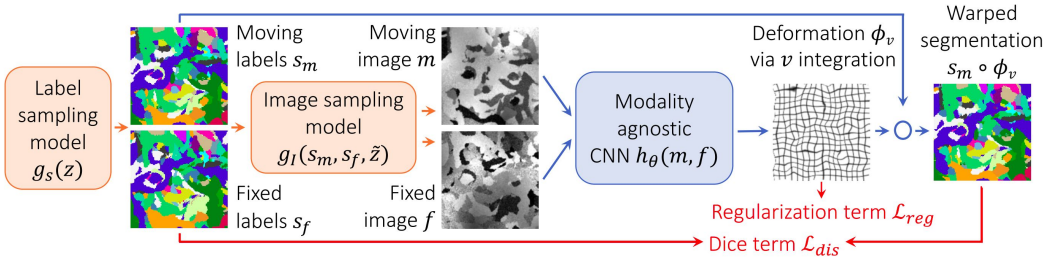

Fig. 5. Unsupervised learning strategy for contrast-agnostic registration. At every mini-batch, we synthesize a pair of 3D label maps $\{s_m, s_f\}$ and the corresponding 3D images $\{m, f\}$ from noise distributions. The label maps are incorporated into a loss that is independent of image contrast. Figure and caption retrieved from original paper in [5]

TABLE I
EXPERIMENT RESULTS FROM GROUPS 1 AND 2. SHOWN ARE TRE (MILLIMETERS) MEAN AND STANDARD DEVIATION VALUES. RANKED IN ASCENDING ORDER FOR COLUMN ALL.

Experiment	Case 1	Case 2	Case 3	Case 4	All
1c	7.610 ± 6.187	11.678 ± 6.535	3.337 ± 2.787	10.335 ± 5.058	**8.242 ± 3.684**
2b	6.686 ± 5.729	13.976 ± 7.584	2.100 ± 1.571	12.499 ± 6.771	8.815 ± 5.472
1b	10.615 ± 6.287	13.440 ± 6.302	3.776 ± 2.918	12.933 ± 4.985	10.191 ± 4.450
1a	13.059 ± 5.943	18.924 ± 5.082	5.358 ± 3.256	19.975 ± 6.159	14.329 ± 6.710
Baseline	26.521 ± 11.498	21.931 ± 6.506	12.626 ± 6.382	29.584 ± 12.924	22.665 ± 7.395

TABLE II
EXPERIMENT RESULTS FROM GROUP 3. SHOWN ARE TRE (MILLIMETERS) MEAN AND STANDARD DEVIATION VALUES. RANKED IN ASCENDING ORDER FOR COLUMN ALL.

Experiment	Case 1	Case 2	Case 3	Case 4	All
3b-II	4.355 ± 2.715	4.218 ± 3.981	1.837 ± 1.260	4.762 ± 1.878	**3.793 ± 1.325**
3b-I	6.117 ± 4.188	5.645 ± 5.393	1.953 ± 1.330	4.557 ± 1.978	4.568 ± 1.861
3c	7.834 ± 5.227	8.574 ± 6.248	2.212 ± 1.541	7.007 ± 4.597	6.407 ± 2.869
3a-I	7.437 ± 5.956	13.785 ± 6.537	3.713 ± 3.122	12.586 ± 4.810	9.380 ± 4.675
3a-II	7.432 ± 6.341	13.907 ± 6.511	3.665 ± 3.160	13.364 ± 5.208	9.592 ± 4.921

And finally, we implemented the last experiment on a single registration performing the three transformations affine, b-spline 1, and b-spline 2, using only the lung mask with CLAHE, and the changes in the registration components from the previous experiment (table III).

- **Final**. Modified parameter 11 affine + b-spline 1 + b-spline 2, using only lung mask and CLAHE.

As per the computation time, for experiments in group 1, they took an average of 2.5 minutes per case image, for group 2, 8 minutes, for group 3, 18.4 minutes, and for group 4, 4.42 minutes. The final experiment took an average of 23.3 minutes per case image.

In figure 6, we see a qualitative example for the case 1 registration using the final experiment settings.

B. Registration using deep learning model

In table IV, we see the results during the inference experiment with our preprocessed dataset. From the model we got back the deformation map with direct and inverse transform, from which we morph the moving image and transform the landmark points, respectively.

- **Baseline**. After the translation + affine registration performed during preprocessing stage.
- **Final**. Models output after morphing the moving image with the predicted deformation map.

TABLE III
EXPERIMENT RESULTS FROM GROUP 4. SHOWN ARE TRE (MILLIMETERS) MEAN AND STANDARD DEVIATION VALUES. RANKED IN ASCENDING ORDER FOR COLUMN ALL.

Experiment	Case 1	Case 2	Case 3	Case 4	All
Final	1.329 ± 1.622	2.525 ± 3.736	1.097 ± 0.999	1.376 ± 1.140	**1.582 ± 0.640**
4d	1.462 ± 1.816	2.542 ± 3.605	1.225 ± 1.050	1.442 ± 1.111	1.668 ± 0.592
4c	1.996 ± 2.540	3.032 ± 4.481	1.354 ± 1.172	1.528 ± 1.136	1.977 ± 0.754
4b	2.578 ± 3.153	3.005 ± 3.951	1.430 ± 1.156	1.681 ± 1.257	2.174 ± 0.742
4a	3.139 ± 4.465	3.476 ± 5.131	1.387 ± 1.169	1.755 ± 1.454	2.439 ± 1.023
4e	2.653 ± 5.335	2.739 ± 3.907	1.133 ± 0.975	10.525 ± 13.468	4.263 ± 4.240

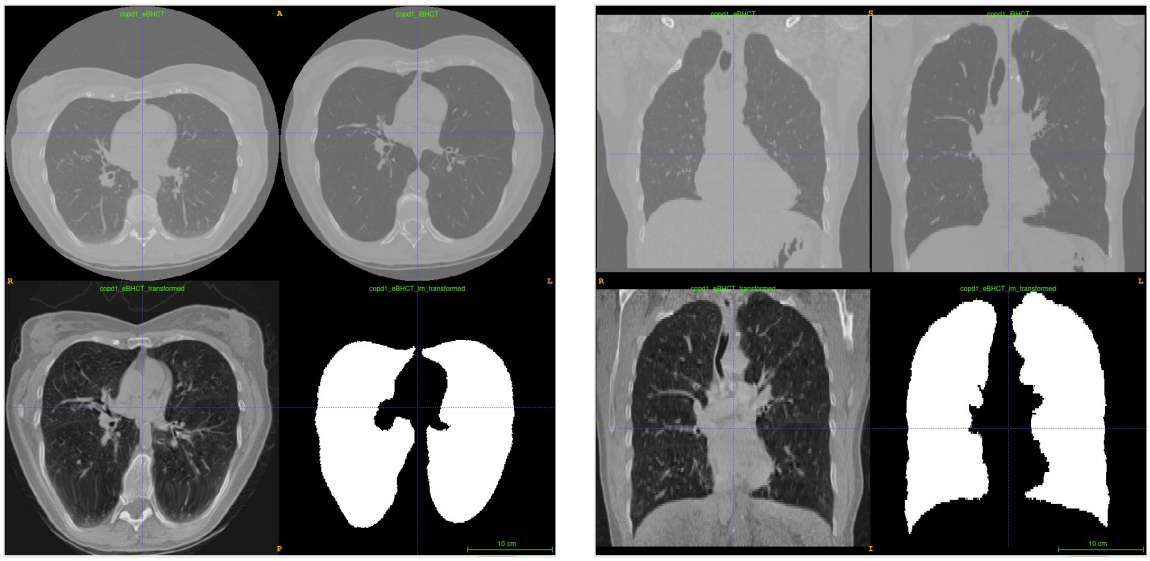

Fig. 6. Registration results for case image 1. Left- axial view, right- coronal view. TL- Original exhale, TR- Original inhale, BL- Registered exhale, BR- Registered lung mask exhale.

TABLE IV
EXPERIMENT RESULTS FROM SYNTHMORPH'S SM-SHAPES MODULE INFERENCE. SHOWN ARE TRE (MILLIMETERS) MEAN AND STANDARD DEVIATION VALUES. RANKED IN ASCENDING ORDER FOR COLUMN ALL.

Experiment	Case 1	Case 2	Case 3	Case 4	All
Final	11.858 ± 17.908	15.318 ± 8.741	12.760 ± 6.865	20.961 ± 10.061	**15.224 ± 4.096**
Baseline	15.051 ± 16.794	18.667 ± 6.712	12.819 ± 6.476	27.418 ± 10.435	18.489 ± 6.422

C. Challenge day

For the day of the challenge, we developed an automated pipeline that receives both the inhale and exhale scans in NIFTI format, as well as the inhale points to be transformed. The framework would pre-process the image, obtain the lung mask from both inhale and exhale scans, perform the registration with the setting of the final experiment, and finally transform the points, exhale image, and lung mask image. The transformed points would be sent to the professor to compute the TRE with the exhale points and finally rank the results of the challenge.

The images available for the challenge were the dataset cases 0, 5, and 6, with case 0 being a more challenging image with poor contrast between tissues. The final results can be seen in table V.

TABLE V
DAY OF THE CHALLENGE RESULTS.

Case	Mean TRE	Lung mask creation time	Registration time	Full pipeline time
Case 0	0.8508 mm	78.82 s	538.45 s	624.3 s
Case 5	1.4985 mm	110.14 s	782.38 s	924.37 s
Case 6	1.9196 mm	106.57 s	727.84 s	867.74 s
Mean total	1.4230 mm	98.5 s	682.89 s	805.47 s

IV. DISCUSSION AND CONCLUSIONS

For the intensity-based registration approach using Elastix, we can conclude that the basic default affine transformation (1a) improves quite considerably the baseline (no registration) TRE. From there, adding a b-spline transformation after the affine lowers the TRE even more. This is due to the fact that affine transformation performs a general image alignment and the non-rigid one refines it (1b, 1c). Nevertheless, using the lung maks for the b-slipe transformation in experiment 2b did not improve further the average results. We believe this happened since we needed to divide the registration into two parts for us to include different masks for each stage, contrary to setting a single mask and a single multi-transformation registration. This phenomenon was perceived in further experiments.

For group 3 of the experiments, we observe that using task-specific parameters improves the registration performance with the correct combination of transformations and masks. For example, experiments 3a-I and II improve the performance compared to their analogous 1b. This got us to conclude that changing the metric and adding more resolutions in the pyramid (amongst other changes of registration components) fits better to our problem, as hypothesized. Moreover, in order to surpass the 1c and 2b performances, it was necessary to use the lung mask with the b-spline after the affine transformation (3b-I and II). In this case, the b-spline parameter maps paired well with the lung mask usage and showed a decrease in TRE. Lastly, even though we tried to implement the pipeline by [10], we didn't manage to make it work, and those results (3c) fell below 3b.

An even more interesting result was seen in experiments from group 4. We decided to use directly the lung mask and a single b-spline transformation to improve computational time and it led to the best results thus far. Because of the large number of experiments to search the optimal registration components, we decided to use this simple registration due to its benefits (low TRE, low computation time).

Finally, by following the learned conclusions from the previous set of experiments, we decided to use the lung mask only in a single multi-transformation registration, with CLAHE preprocessing, and tuned parameter maps, thus leading to the lowest TRE.

For future work, it would be proper to implement further the idea of a non-intensity similarity metric, based on gradient information, such as the normalized gradient fields (NGF) [4]. In this way, the rich structure exhibited by the lungs (bronchi, vessels, fissures, etc.) can be exploited. Also, in our registration pipeline we never formally addressed the sliding motion phenomenon that occurs in the thorax with the inhaling and exhaling phases of the lungs [8]. We did not consider it because our performance metric based on landmarks was focusing only on the lungs, but it should be considered when the border between the lungs and rib cage is important.

Regarding the deep learning registration approach, there are many models to try and thankfully some authors have shared their code publicly. Even by taking advantage of this, adapting the models to our specific tasks requires a lot of time. And in our case, time played against us. The obtained results show interesting performance with the novel contrast-agnostic-trained models, but they require further tuning and adaptation. Despite improving the TRE compared to the initial values or the baseline (rigid and affine) registration, the results of the shapes SynthMorph were far below the results of the best Elastix pipeline we implemented. One way of adopting the SythMorph shape model to the task of lung CT registration, and thus improving its results, would be a fine-tuning of the model based on the lung CT images. It could be done with either a registration-based similarity metric between the target and moving images based on the predicted deformation field, or exploiting the key points and incorporating a TRE into the cost function directly as an additional term. We believe this idea could be a basis for interesting future research into the applicability of such general models and the prospect of their adaptation to specific registration tasks.

REFERENCES

[1] Richard Castillo et al. "A reference dataset for deformable image registration spatial accuracy evaluation using the COPDgene study archive". In: *Physics in Medicine Biology* 58.9 (Apr. 2013), p. 2861. DOI: 10.1088/0031-9155/58/9/2861. URL: https://dx.doi.org/10.1088/0031-9155/58/9/2861.

[2] Lasse Hansen and Mattias P. Heinrich. "GraphRegNet: Deep Graph Regularisation Networks on Sparse Keypoints for Dense Registration of 3D Lung CTs". In: *IEEE Transactions on Medical Imaging* 40.9 (2021), pp. 2246–2257. DOI: 10.1109/TMI.2021.3073986.

[3] Mattias P. Heinrich and Lasse Hansen. “Going beyond the cranial vault with keypoint supervision and multi-channel instance optimisation [Unpublished]”. In: *arXiv* 2203.00046v1 (2022). DOI: 10.48550/arXiv.2203.0004. URL: https://doi.org/10.48550/arXiv.2203.00046.

[4] Alessa Hering et al. “CNN-based lung CT registration with multiple anatomical constraints”. In: *Medical Image Analysis* 72 (2021), p. 102139. ISSN: 1361-8415. DOI: https://doi.org/10.1016/j.media.2021.102139. URL: https://www.sciencedirect.com/science/article/pii/S1361841521001857.

[5] Malte Hoffmann et al. “SynthMorph: learning contrast-invariant registration without acquired images”. In: *IEEE Transactions on Medical Imaging* 41.3 (2022), pp. 543–558.

[6] Johannes Hofmanninger et al. “Automatic lung segmentation in routine imaging is primarily a data diversity problem, not a methodology problem”. In: *European Radiology Experimental* 4.1 (2020). DOI: 10.1186/s41747-020-00173-2.

[7] *Information on COPD*. URL: https://www.copdgene.org/information-copd.htm.

[8] Laurent Risser et al. “Piecewise-diffeomorphic image registration: Application to the motion estimation between 3D CT lung images with sliding conditions”. In: *Medical Image Analysis* 17.2 (2013), pp. 182–193. ISSN: 1361-8415. DOI: https://doi.org/10.1016/j.media.2012.10.001. URL: https://www.sciencedirect.com/science/article/pii/S1361841512001466.

[9] Jan Rühaak et al. “Estimation of Large Motion in Lung CT by Integrating Regularized Keypoint Correspondences into Dense Deformable Registration”. In: *IEEE Transactions on Medical Imaging* 36.8 (2017), pp. 1746–1757. DOI: 10.1109/TMI.2017.2691259.

[10] Marius Staring et al. “Pulmonary Image Registration with elastix using a Standard Intensity-Based Algorithm”. In: *Book pulmonary image registration with elastix using a standard intensity-based algorithm* (Jan. 2010).